

# Sensor Planning for PTZ Cameras Using the Probability of Camera Overload

Yi Yao, Chung-Hao Chen, Besma Abidi, David Page, Andreas Koschan, and Mongi Abidi  
*Imaging, Robotics and Intelligent Systems (IRIS) Lab*  
*University of Tennessee, Knoxville*

## Abstract

*Most existing sensor planning algorithms find it difficult to tackle the discrepancy between a PTZ camera's limited instant field of view (FOV) and panoramic achievable FOV. In this paper, we introduce the probability of camera overload to resolve this discrepancy and present a sensor planning algorithm for PTZ cameras under the same framework as static cameras. The resulting camera placement achieves the optimal balance between coverage and handoff success rate. Furthermore, our algorithm is able to incorporate the target's dynamics into sensor planning. As a result, the system's handoff success rate can be maintained in environments with various target densities. Experimental results and comparisons with a reference algorithm proposed by Erdem and Sclaroff verify the effectiveness of our algorithm via a significantly improved handoff success rate.*

## 1. Introduction

With the increased scale and complexity involved in most practical surveillance applications, it is almost impossible for any single camera (either omnidirectional or PTZ) to fulfill tracking and monitoring with an acceptable degree of continuity and/or a reasonable accuracy. Systems with multiple cameras find extensive applications in these situations. The concept of sensor planning comes naturally when the question of how to place multiple cameras for the best coverage and at the lowest cost arises.

In literature, most sensor planning algorithms are proposed for such applications as 3D object inspection and reconstruction [1-3]. Sensor planning for surveillance systems also received increasing attention in recent years [4, 5]. Cameras are placed such that a full or specified coverage of the environment or object is achieved. A probabilistic camera planning framework with visibility analysis of dynamic occlusions was proposed by Mittal and Davis [6]. Erdem and Sclaroff defined different types of

coverage problems and developed corresponding solutions [7]. The conventional requirements in sensor planning, such as coverage and visibility, are unable alone to ensure an automated tracking in real-time surveillance systems. A uniform and sufficient amount of overlap between the FOVs of adjacent cameras should be reserved so that consistent labeling and camera handoff can be executed successfully. Sensor planning algorithms achieving the optimal balance between coverage and handoff success rate are discussed for static perspective cameras in [8].

However, most existing sensor planning algorithms find it difficult to properly model PTZ cameras. Let the instant FOV denote the FOV that a PTZ camera can see at any given time instance and the achievable FOV the FOV that a PTZ camera can survey given a sufficient period of time. The camera's limited pan and tilt speeds lead to the discrepancy between the instant and achievable FOVs, which in consequence introduces difficulties in modeling PTZ cameras for sensor planning. Some algorithms simply use the achievable FOV for the sensor planning of PTZ cameras. Erdem and Sclaroff defined the reachable region to model PTZ cameras [7]. It is assumed that a PTZ camera has two end points for panning. The reachable region corresponds to the intersection areas that the PTZ camera can pan from these two end points during a given period of time. The reachable region represents the camera's coverage in the worst case since these two end points are the farthest points in the camera's achievable FOV. This may result in a camera placement with excessive overlapped achievable FOVs.

In this paper, we extend our previous work regarding static perspective cameras to PTZ cameras by introducing the probability of camera overload. The significance of deriving the probability of camera overload is two-folded. (1) It solves the discrepancy between the PTZ camera's instant and achievable FOVs and provides the optimal placement from a statistical perspective. In comparison, Erdem and Sclaroff's method is able to provide a sensor placement in the worst case scenarios depending on

the starting point of pan and the given period of time. (2) The target's dynamics are incorporated into sensor planning. The optimal camera placement is obtained according to the targets' statistical distribution in the environment. More overlapped FOVs are secured for more clustered environments so that the target has more freedom to be transferred to another camera when experiencing camera overload or dynamic occlusion. On the contrary, the sensor placement generated from Erdem and Sclaroff's method only depends on the environment's geometry but disregards the target's dynamics.

The remainder of this paper is organized as follows. The sensor planning algorithm for PTZ cameras is described in Section 2. Section 3 derives the probability of camera overload. Section 4 presents our experimental results and Section 5 concludes the paper.

## 2. Sensor planning

Figure 1 illustrates the flow chart of the proposed sensor planning algorithm. Given the  $i^{\text{th}}$  grid on the floor plan and the  $j^{\text{th}}$  camera's parameters, observation measure  $Q_{ij}$  is computed to describe the suitability of the  $i^{\text{th}}$  grid observed by the  $j^{\text{th}}$  camera. Meanwhile, the probability of camera overload at the  $i^{\text{th}}$  grid  $P_{co,i}$  describing the probability that all the observing cameras have reached the maximum computational load is evaluated. Based on  $Q_{ij}$  and  $P_{co,i}$ , the objective function  $c_i$  of the  $i^{\text{th}}$  grid is formulated and used to guide the search of the optimal camera parameters  $T_{C,j}$ .

Assume that a polygonal floor plan is represented as an occupancy grid. The  $j^{\text{th}}$  camera is placed at  $T_{C,j} = [T_{X,j} \ T_{Y,j} \ T_{Z,j}]^T$  and the coordinates of the  $i^{\text{th}}$  grid on the floor plane are  $G_i = [G_{X,i} \ G_{Y,i}]^T$ . The observation measure of the  $i^{\text{th}}$  grid from the  $j^{\text{th}}$  camera is defined as:

$$Q_{ij} = 1 - \frac{(G_{X,i} - T_{X,j})^2 + (G_{Y,i} - T_{Y,j})^2 + T_{Z,j}^2}{R_o^2}, \quad (1)$$

where  $R_o$  denotes the maximum observation distance.

A failure threshold  $Q_F$  and a trigger threshold  $Q_T$  are derived to define three disjoint regions: (1) invisible area with  $Q_{ij} < Q_F$ , (2) visible area with  $Q_{ij} \geq Q_T$ , and (3) handoff safety margin with  $Q_F \leq Q_{ij} < Q_T$ . The derivation of the failure threshold  $Q_F$  is straightforward due to the way the observation measure is defined. According to (1),  $Q_{ij}$  varies between zero and one if the  $i^{\text{th}}$  grid is within

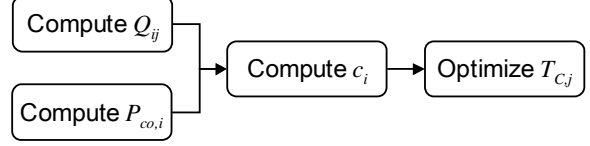


Figure 1. Flow chart of the proposed sensor planning algorithm.  $Q_{ij}$ : the observation measure of the  $i^{\text{th}}$  grid from the  $j^{\text{th}}$  camera.  $P_{co,i}$ : the probability of camera overload of the  $i^{\text{th}}$  grid.  $c_i$ : the objective function of the  $i^{\text{th}}$  grid.  $T_{C,j}$ : the parameter of the  $j^{\text{th}}$  camera.

the observation distance of the  $j^{\text{th}}$  camera.  $Q_{ij}$  has negative values if the  $i^{\text{th}}$  grid is beyond the observation distance the  $j^{\text{th}}$  camera. Therefore,  $Q_F$  can be simply set to zero. The trigger threshold  $Q_T$  is given by  $Q_T = Q_F + \kappa u_{obj} t_H$  where  $u_{obj}$  represents the average moving speed of the object of interest,  $t_H$  denotes the average duration for a successful handoff, and  $\kappa$  is a conversion scalar.

Let  $A_C$  represent the grid coverage with  $a_{C,ij} = 1$  if  $Q_{ij} \geq Q_F$  and  $a_{C,ij} = 0$  otherwise. We also define matrix  $A_H$  with  $a_{H,ij} = 1$  if  $Q_F \leq Q_{ij} < Q_T$  and  $a_{H,ij} = 0$  otherwise and matrix  $A_V$  with  $a_{V,ij} = 1$  if  $Q_{ij} \geq Q_T$  and  $a_{V,ij} = 0$  otherwise. Matrices  $A_H$  and  $A_V$  represent the handoff safety margin and visible area, respectively. Let  $\mathbf{c}'_C = A_C \mathbf{x}$ ,  $\mathbf{c}'_H = A_H \mathbf{x}$ , and  $\mathbf{c}'_V = A_V \mathbf{x}$ , where the solution vector  $\mathbf{x}$  specifies a set of chosen camera configurations with the corresponding element  $x_j = 1$  if the configuration is chosen and  $x_j = 0$  otherwise. The objective function for sensor planning is formulated as:

$$c_i = w_C (c'_{C,i} > 0) + w_H (c'_{H,i} = 2) - w_V (c'_{V,i} > 1) + w_{co} (P_{co,i} \leq P_{co,th})', \quad (2)$$

where  $w_C$ ,  $w_H$ ,  $w_V$ , and  $w_{co}$  are predefined importance weights,  $P_{co,i}$  denotes the probability of camera overload at the  $i^{\text{th}}$  grid, and  $P_{co,th}$  a predefined threshold. The definition of the probability of camera overload will be given in Section 3. The operation

$(c'_{C,i} > 0)$  means  $(c'_{C,i} > 0) = \begin{cases} 1 & c'_{C,i} > 0 \\ 0 & otherwise \end{cases}$ . The

first term in the objective function considers coverage, the second term produces sufficient overlapped handoff safety margins, and the third term penalizes excessive overlapped visible areas. Our objective function achieves a balance between coverage and sufficient margins for camera handoff. The fourth term minimizes the probability of a



and a PTZ camera are  $N_{obj,j} \geq 1$  and  $N_{obj,j} = 1$ , respectively. Furthermore, the computation of the probability of camera overload depends on the target's arrival rate and residence time, which describes the target's dynamic distribution in the environment. The resulting optimal camera placement not only depends on the environment's geometry but also adjusts to the target's dynamics.

#### 4. Experimental results

Experiments are conducted using indoor and outdoor floor plans with various scales. Since similar observations are achieved, due to limited space, experimental results using one typical indoor office floor plan with dimensions of 20m×15m are presented and compared in this paper with a leading algorithm proposed by Erdem and Sclaroff [7]. Two criteria are used to evaluate and compare their performances: coverage and handoff success rate. Handoff success rate, the ratio between the number of successful handoffs and the number of requested handoffs, is an important performance measure for automated surveillance systems. A successful camera handoff between adjacent cameras ensures that the same target maintains the same identity across different cameras' FOVs.

To obtain a statistically valid estimation of the handoff success rate, simulations are carried out to enable a large amount of tests under various conditions. A pedestrian behavior simulator [9, 10] is implemented so that we could achieve a close resemblance to experiments in real environments and in turn an accurate estimation of the handoff success rate. Several points of interest are generated randomly to form a pedestrian trace. The handoff success rate is obtained from simulation results of 300 randomly generated traces. The arrival of the pedestrian follows a Poisson distribution. The average walking speed is 0.5m per second.

Since one major advantage of our algorithm is the consideration of targets' statistical distribution, we focus on testing and comparing the algorithms' performances in environments with a variety of target densities. In theory, given the proper estimation of the target density in the environment, the same value should be used in sensor planning. However, in our experiment, we purposefully use two sets of arrival rates. One set of arrival rates is used in sensor planning. Three camera placements are generated with  $\lambda=0.01$ , 0.025, and 0.05, representing environments with low, medium, and high target

density, respectively. The other set is used in the simulation of target behavior. The tested arrival rates vary from 0.01 to 0.05, resulting in a maximum number of targets in the range from one to six. We employ different values of target arrival rates to verify that the camera placement with a certain arrival rate is able to maintain the handoff success rate for environments with an arrival rate up to that value used in sensor planning.

Figure 3 illustrates and compares our experimental results. Figures 3(b)-(d) show the camera placement obtained from our method with different target densities. Note that the optimization of the camera's parameters is not restricted to 2D. The optimized position of a PTZ camera includes both  $T_x/T_y$  and  $T_z$  (height). For clear presentation, Figures 3(b)-(d) illustrate the FOVs of the cameras at the optimal positions that are projected onto the 2D ground plane. A larger arrival rate/target density setting leads to a camera placement with more overlapped FOVs between adjacent cameras so that the tracked target has more freedom to be transferred to another camera when experiencing dynamic occlusion and/or camera overload.

The advantage of our method over the reference method becomes conspicuous when we look into the handoff success rate with respect to the maximum number of targets in the environment, as shown in Figure 3(e). When the maximum number of targets is one, our method elevates the handoff success rate from 48.7% to 100% and maintains a similar coverage. As the maximum number of targets in the environment increases from one to six, the handoff success rate of the reference method drops gradually from 48.7% to 10.2%. On the contrary, the handoff success rate of our method is maintained within 90% for camera placement with  $\lambda=0.025$  ( $\lambda=0.05$ ) till the maximum number of targets reaches four (six). As expected, with different density parameters used in (6) and (7), the resulting camera placement yields different capacity in handling clustered environments. In our experiments,  $\lambda=0.025$  and  $\lambda=0.05$  corresponds to an environment with a maximum number of targets of approximately four and six, respectively. The resulting sensor placement can maintain the handoff success rate till the maximum number of targets reaches four and six, respectively. Therefore, the proposed algorithm is able to achieve and maintain a significantly higher handoff success rate according to the targets' density in the environment.

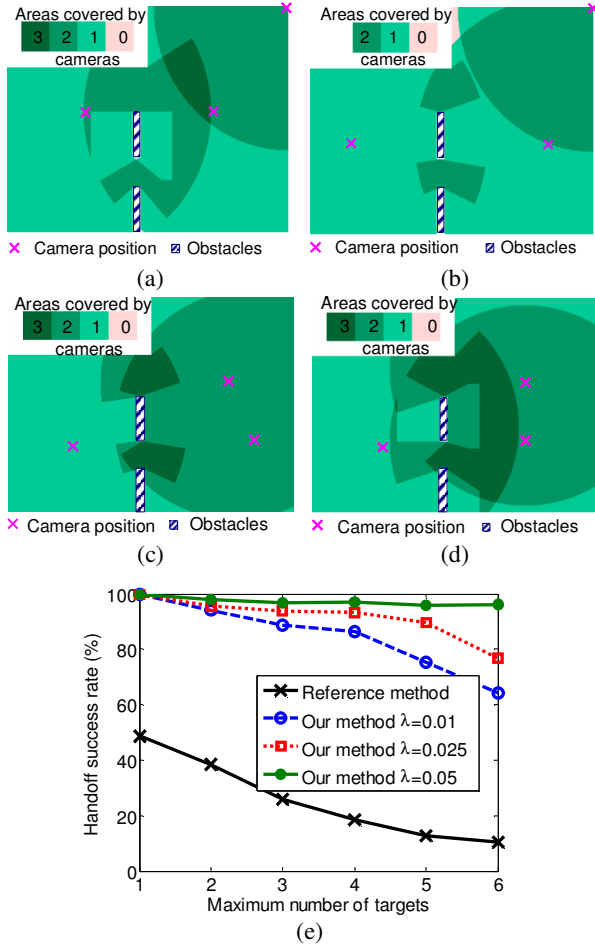


Figure 3. Sensor planning results for PTZ cameras considering various target densities. The optimal camera positioning using PTZ cameras: (a) the reference method (coverage: 100.0%), (b) our method with  $\lambda=0.01$  (coverage: 99.5%), (c) our method with  $\lambda=0.025$  (coverage: 100.0%), and (d) our method with  $\lambda=0.05$  (coverage: 100.0%). (e) System performance comparison based on handoff success rate with various target densities. The target density is described by the maximum number of targets to be tracked simultaneously in the environment.

## 5. Conclusions

A sensor planning algorithm designed for PTZ cameras that is able to achieve the optimal balance between coverage and handoff success rate was proposed. The probability of camera overload was derived and employed to solve the discrepancy between a PTZ camera's instant and achievable FOVs. The proposed sensor planning algorithm not only considers the PTZ camera's dynamics from panning and tilting but also incorporates the target's dynamics. Experimental results demonstrated a significantly improved handoff success rate in

comparison with the reference algorithm described by Erdem and Sclaroff in environments with various target dynamics.

## Acknowledgements

This work was supported in part by the University Research Program in Robotics under grant DOE-DE-FG52-2004NA25589.

## References

- [1] S. D. Roy, S. Chaudhury, and S. Banerjee, "Recognizing large isolated 3-D objects through next view planning using inner camera invariants", *IEEE Trans. on Systems, Man and Cybernetics*, vol. 35, no. 2, pp. 282-292, Apr. 2005.
- [2] L. M. Wong, C. Dumont, and M. A. Abidi, "Next best view system in a 3D object modeling task", *IEEE Int'l Symposium on Computational Intelligence in Robotics and Automation*, Monterey, CA, Nov. 1999, pp. 306-311.
- [3] S. Yous, N. Ukita, and M. Kidode, "Multiple active camera assignment for high fidelity 3D video", *IEEE Int'l Conf. on Computer Vision Systems*, New York, Jan. 2006.
- [4] F. Z. Quereshi and D. Teropoulos, "Towards intelligent camera networks: a virtual vision approach", *IEEE Int'l Workshop on Visual Surveillance and Performance Evaluation of Tracking and Surveillance*, Beijing, China, Oct. 2005, pp. 177-184.
- [5] Q. Cai and J. K. Aggarwal, "Tracking human motion in structured environments using a distributed-camera system", *IEEE Trans. on Pattern Recognition and Machine Intelligence*, vol. 21, no. 11, pp. 1241-1247, Nov 1999.
- [6] A. Mittal and L. S. Davis, "Visibility analysis and sensor planning in dynamic environments", *European Conf. on Computer Vision*, Prague, Czech Republic, May 2004, pp. 175-189.
- [7] U. M. Erdem and S. Sclaroff, "Automated camera layout to satisfy task-specific and floor plan-specific coverage requirements", *Computer Vision and Image Understanding*, vol. 103, no. 3, pp. 156-169, Sept. 2006.
- [8] Y. Yao, C.-H. Chen, B. Abidi, D. Page, A. Koschan, and M. Abidi, "Sensor planning for automated and persistent object tracking with multiple cameras", *IEEE Conf. on Computer Vision and Pattern Recognition*, Anchorage, AK, Jun. 2008.
- [9] G. Antonini, S. Venegas, M. Bierlaire, and J. Thiran, "Behavioral priors for detection and tracking of pedestrians in video sequences", *Int'l Journal of Computer Vision*, vol. 69, no. 2, pp. 159-180, Aug. 2006.
- [10] J. Pettre, T. Simeon, and J. P. Laumond, "Planning human walk in virtual environments", *IEEE/RSJ Int'l Conf. on Intelligent Robots and Systems*, Lausanne, Switzerland, Sept. 2002, pp. 3048-3053.